Optimal Sizing of a PV-Battery Stand-Alone Fast Charging Station for Electric Vehicles Using SO

Abd El-Fattah A. Omran*‡, Abd El-Shafy A. Nafeh*‡, Hosam K. M. Yousef **

* Electronics Research Institute (ERI), Cairo, Egypt

** Faculty of Engineering, Cairo University, Giza, Egypt

(abdo_omran90@yahoo.com, abdoomran@eri.sci.eg, abdelshafyn@yahoo.com, abdelshafyn@eri.sci.eg, Hosamkm@eng.cu.edu.eg)

‡ Corresponding Author1; Abd El-Fattah A. Omran, abdo_omran90@yahoo.com, abdoomran@eri.sci.eg

‡ Corresponding Author2; Abd El-Shafy A. Nafeh, abdelshafyn@yahoo.com, abdelshafyn@eri.sci.eg

Received: 27.09.2022 Accepted: 02.11.2022

Abstract- This paper proposes a methodology for the optimal sizing of a complete green photovoltaic (PV)-battery stand-alone fast charging station for electric vehicles (FCSEVs) in Cairo, Egypt. The formulated optimization problem aims to minimize the total system cost and ensure the high reliability of the proposed system; by obtaining the optimal numbers of the utilized PV modules (N_{PV}) and battery storage units (N_B). At the same time, it aims to maximize the overall system profit; by selling the energy to electric vehicles (EVs). Also, a comparison among the proposed MATLAB-based snake optimization algorithm, which is simply called snake optimizer (SO), and some other meta-heuristic optimization algorithms, such as Grey Wolf Optimizer (GWO), Particle Swarm Optimization (PSO), and Genetic Algorithm (GA), is conducted, in this work, to verify the feasibility of the proposed optimization algorithm in satisfying the desired ultimate goals of the sizing of the considered stand-alone system. In addition, a techno-economic study is conducted to assess the economic viability of the proposed optimum system over the project lifetime. The obtained results showed that the proposed energy management strategy is effective in controlling the energy flow within the proposed system. In addition, they indicated that the proposed SO can give the best optimization results compared to the other considered algorithms. Finally, the obtained results showed, also, that the integration of the stand-alone PV-battery in FCSEVs is crucial and necessary to overcome the well-known problems of the conventional fossil fuel resources.

Keywords: Photovoltaic; Battery storage system; Electric vehicles; Charging stations; Snake optimization.

1. Introduction

Nowadays, the rapid development of electric vehicle (EV) technologies is due to rising environmental concerns and technological advancements in power electronics and energy storage. Large-scale deployment of EVs in the transportation sector has the potential to reduce greenhouse gas emissions and, also, to increase the contribution of renewable energy resources in the transportation sector, which in turn can reduce the overall dependance on fossil fuel resources [1-3]. Since EVs depend entirely on the electricity stored in their batteries, an increase in the availability of public EV charging stations (EVCSs) is crucial for the widespread utilization of these vehicles [1]. At the same time, these EVCSs must be widely distributed, so that EV owners can confidently travel long distances with easy access to recharging facilities whenever needed.

By 2025, it is expected that there will be over 10 million EVs on the roads worldwide [4, 5]. Also, it is expected to reach 1.3 million public EV chargers by 2025, and 2.9 million by 2030 [6].

Due to the depletion of fossil fuels, concerns about weather change, the importance of energy divergence, and the potential for the creation of jobs, many governments are embracing renewable energy as part of their energy portfolios. Considering the high-costs related with network expansion, the use of renewable energy technologies as self-sustaining energy systems would be economically feasible and affordable in many remote locations throughout the world [7].

One reason for the recent spread of EVs in Egypt is the state's efforts to encourage citizens to buy EVs instead of internal combustion engine vehicles to reduce pollution. Noting that the current exemption of EVs from customs and taxes in Egypt, as well as the availability of their charging stations (CSs) will contribute to the growth of their owners in Egypt in the near future. In addition, the Egyptian government encourages this trend by putting an ambitious plan to build 6000 public EV CSs in the near future.

The integration of renewable energy sources (RESs) such as photovoltaic (PV) with battery storage systems (BSSs) can mitigate the intermittence nature of RESs' output power and meet the requirements of charging the EVs with the required acceptable reliability [8-10]. With the BSS integration, the surplus power generated by the PV modules during the daytime can be stored. The BSS then releases the stored energy when the incident insolation on the PV modules is in sufficient or there is a deficit in the PV output power (i.e., during the evenings) [11, 12].

The main challenges that face the adaptation of EVs are their limited driving range, their high battery replacement costs, and their long charging time [13]. The first two obstacles have been overcome by the developed technologies of lithium-ion batteries that could provide the EVs's owners with large storage capacities at reduced costs. Also, fast charging stations (FCS) have recently been used to overcome the last issue of long charging time. Where, the FCS can restore the charging of an EV to about 80% of its state of charge (*SOC*) within half an hour of its depletion [4]. However, the fast charging techniques require high power demand to reduce the long charging time.

The stand-alone CSs are not connected to the grid and their energy requirements are commonly met using distributed energy resources (DERs), which may include renewables, non-renewables [14], or a combination of them. These kinds of CSs are the best solution for remote areas that lack adequate connectivity to the power grid. Additionally, because stand-alone CSs must meet load demand during operation, they require careful and comprehensive investigations [15, 16].

Currently, the optimal techno-economical design of stand-alone PV-battery systems for charging EVs is essential for ensuring their economic viability, which necessitates the sizing of system components at the lowest cost. In reality, a well-designed stand-alone PV-battery system helps to avoid power outages, ensure the quality and security of the power supply, and achieve economic and environmental benefits [17].

Recently, many studies have been conducted on the sizing of stand-alone charging stations for EVs (CSEVs). In [15], a robust optimization technique was proposed for sizing a PV-diesel-fuel cell stand-alone CS that would provide electricity to EVs and hydrogen to hydrogen vehicles (HVs). In [17], the technical and economic viability of a stand-alone PV-battery storage system for EVs charging in Madrid, Spain was analyzed and conducted by using HOMER software and by taking into account the principle of load shifting. The results indicated that the designed system was technically and economically viable and reliable. Also, they indicated that the designed system can significantly reduce air pollution and is profitable. A methodology for determining the optimal sizing of stand-alone PV-battery CSEV, that aims to reduce the system investment costs while achieving the CS's performance metrics, was presented in [18]. In [19], the optimal sizing of a PV-wind-battery stand-alone CSEV was presented using HOMER software. This system could produce an annual energy of 843.15 MWh with an electricity cost of 0.064 $/kWh.

Using Simulink design optimization, an optimal method for sizing a PV-wind-battery stand-alone microgrid (MG), that can transfer wireless power for electrical and hydrogen CSs of EVs and fuel cell-powered buses, respectively, on a highway, was proposed in [20].

Using a multi-objective PSO algorithm, the optimal sizing of the PV-wind-battery system in two different scenarios (i.e., with and without EV) was investigated in [21]. In the first scenario, (i.e., PV-wind-battery), the optimal number of system components and cost are determined at various levels of reliability (i.e., loss of power supply probability (*LPSP*)). Then, in the second scenario, an EV is added to the system (i.e., PV-wind-battery-EV) and the *LPSP* is recalculated under both deterministic and stochastic conditions. The outcomes proved that the design of both systems is feasible. However, the first system was more efficient as it utilized fewer wind turbines in a greater number of identical values of *LPSP*.

In order to obtain the optimal configuration and meet the daily charging demand, a techno-economic analysis of a novel RESs-based stand-alone CS is conducted in [22], by using HOMER software and by using the different geographical and metrological conditions of four Qatari cities. In each location,

a comprehensive economic criterion was used to compare the obtained optimal solution with the grid extension option. The findings indicated that the proposed optimization method can be used anywhere, given the site's metrological conditions.

The study in [23], proposed and thermos-dynamically assessed a stand-alone CSEV that comprises concentrated photovoltaic–thermal (CPV/T)-wind-biomass combustion-based steam Rankine-cycle plant. Fuel cells-based hydrogen and ammonia are incorporated into the design to guarantee uninterrupted charging services during the night and in adverse climatic conditions. Based on the findings, 80 EVs can be fast charged daily with the power generated by RESs and fuel cells.

A method for joint capacity optimization of a PV-wind-diesel-battery standalone system, including EV charging load, was presented in [24]. The optimization problem was solved to minimize the system cost, reduce the GHG emissions, and reduce the dumped energy. Also, the optimization problem was solved for different system combinations to determine the most effective and economical load-serving combination. This study may serve as a useful road map for decision-makers, analysts, and policymakers.

In [25], a mixed-integer linear programming (MILP) algorithm was proposed to determine the optimal sizing of PV-battery in a stand-alone nanogrid. The formulated problem is solved using a robust optimization technique. Case studies illustrate the benefits of the proposed applications and validate the considered methodology.

In this paper, a SO optimization algorithm is used to optimally size a proposed stand-alone PV-battery FCSEVs. The main aims of the optimization technique are to minimize the total system cost and ensure the high reliability of the system. The utilized SO optimization algorithm is compared with other meta-heuristic algorithms to verify the robustness of the proposed algorithm over other algorithms in satisfying the desired ultimate goals of the sizing process. Additionally, a techno-economical analysis is conducted to assess the economic viability of the proposed system.

The rest of this paper is structured as follows: Section 2 clarifies the structure of the proposed PV-battery stand-alone FCSEVs. Section 3 presents the metrological and load data used in this study. Section 4 is dedicated for the basic economic background. Section 5 presents the formulation of the optimization problem. Section 6 presents the life cycle cost estimation of the proposed FCSEVs. Section 7 provides the mathematical modelling of the proposed system. Section 8 is dedicated for the proposed energy management strategy and system reliability of the proposed PV-battery stand-alone FCSEVs. Section 9 presents the optimization problem in its final form and SO algorithm. Section 10 illustrates the obtained results of this work. Finally, section 11 provides the concluding remarks.

2. Structure of the PV-Battery Stand-Alone FCSEVS

The structure of the proposed PV-battery stand-alone FCSEVs is shown in Fig. 1, which comprises of a PV source, a battery storage, a conditioning DC-DC and DC-AC converters, and the total load of the station. The total load of the station comprises the base load of the station (e.g., lighting, PC, etc.) and the EVs load. The base load of the station is connected to the AC-side of the DC-AC converter of the system, whereas the EVs load is connected to the common DC bus of the system by using DC-DC converters.

The utilized boost DC-DC converter that is attached to the PV array is to perform the array maximum power point tracking (MPPT). Also, the battery storage is used to grantee the continuity of supplying the station total load with electricity during nights and/or periods of deficit of the available PV energy. Where, the excess PV power that is generated during periods of high insolation levels can be stored in the battery storage for later use. Noting that each converter of the system has its own local control unit that can perform the required control task corresponding to its position. At the same time, the utilized central control unit is used to supervisory control and manage the overall system.

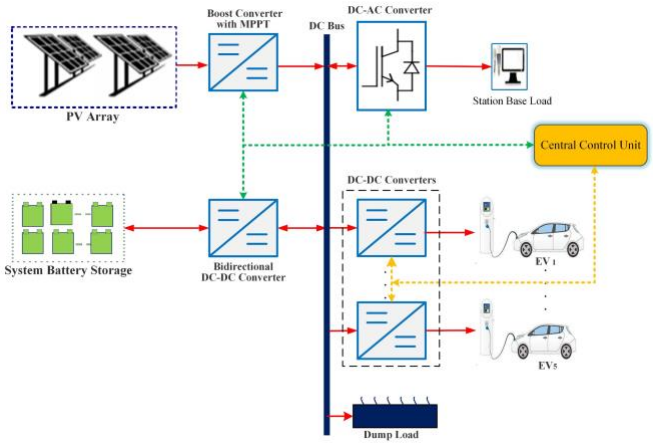

Fig. 1. Structure of the proposed PV-battery stand-alone FCSEVs.

3. Metrological and Load Data

The selected site for the proposed FCSEVs is the New Nozha, Cairo, Egypt. The considered site has a latitude of 30° 5' N and a longitude of 31° 20' E. Figure 2 shows the long-term monthly average daily solar insolation data of the

considered site, which provided by NASA surface meteorology and solar energy database [26]. By using the HOMER Pro software, these data were converted into an hourly average form over one typical year. The annual average solar insolation of the selected site is 6.37 kWh/m^2/day.

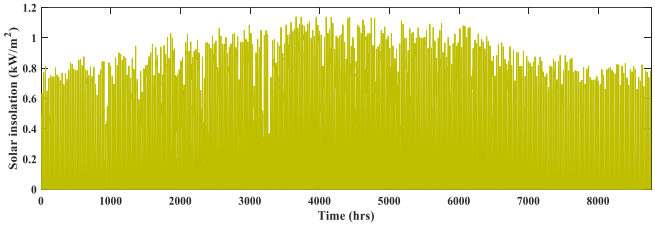

Fig. 2. Solar insolation data for a typical year on hourly basis.

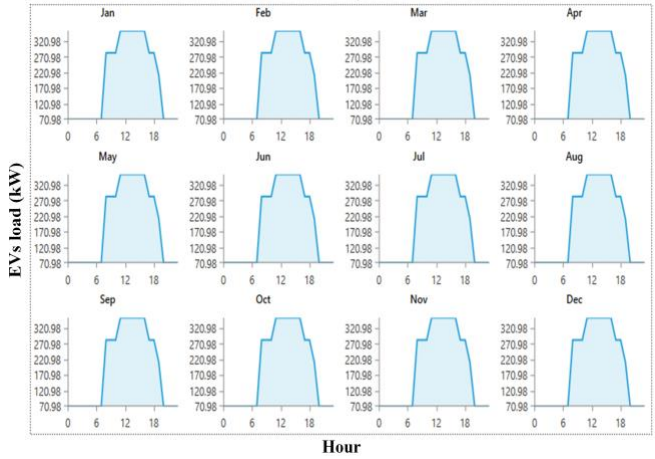

Fig. 3. The EVs load profile of a typical year.

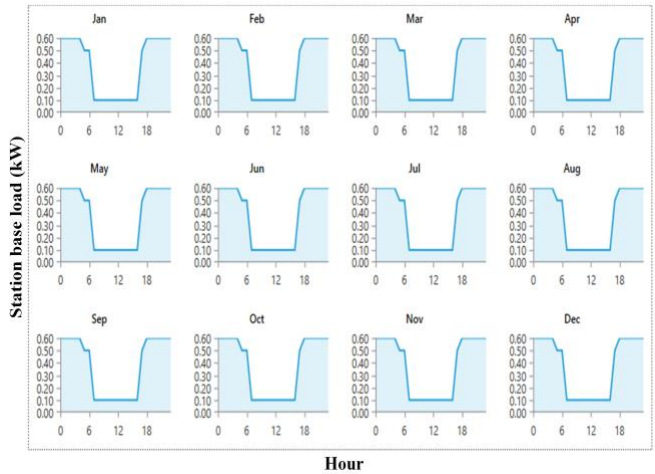

Fig. 4. The station base load profile of a typical year.

The considered EVs load and the station base load profiles during the 12 months of the year are shown, respectively, in Figs. 3 and 4. In this work, the EVs load profile is mainly formed based on the utilization of batteries for the EVs having a capacity of 50.7 kWh each.

4. Basic Economical Background

Generally, there are some important common indicators that can be used to decide the economic feasibility of any renewable energy-based project. These indicators are the life cycle cost (LCC), levelized cost of energy ($LCOE$), and payback period (T_{PB}). The LCC parameter is commonly used to examine the financial impact of the project, i.e., it serves as a guide for selecting the optimal system configuration. The $LCOE$ parameter is used to determine the required cost of electrical energy generated from the project. Also, the T_{PB} is used to measure the profitability of the project [27].

4.1 Life Cycle Cost

The *LCC* (sometimes referred to as the net present cost (NPC), net cash flow, or total system cost (C_T)) of a renewable energy-based project is the total cost of owning and operating all components of the project (i.e., the total capital cost of the project) minus all the revenues that are earned over the project lifetime expressed in today's money. Therefore, generally, the *LCC* is the sum of the present worths (PWs) of all the costs included in the system (e.g., initial capital costs, replacement costs, operation and maintenance costs (O&M), fuel costs, emissions penalty costs, and costs of purchasing electrical energy from the grid) minus all the revenues of all salvage values and selling electrical energy to the grid and/or all different consumers.

Thus, for the considered PV-battery stand-alone FCSEVs, the *LCC* can be expressed as follows

$$LCC = \sum_{k=1}^{K}\left(I_k + R_{k\,PW} + OM_{k\,PW} - S_{k\,PW}\right) - C_{EVs\,PW} \qquad (1)$$

where K is the total number of components included in the system (i.e., PV, system battery storage, DC-DC converters, and DC-AC converter), I_k is the initial capital cost of component k, $R_{k\,PW}$ is the PW of the replacement cost of component k, $OM_{k\,PW}$ is the PW of the O&M cost of component k, and $S_{k\,PW}$ is the PW of the salvage value of component k at the end of its lifetime, and $C_{EVs\,PW}$ is the PW of the cost of the electrical energy sold to EVs.

Equation (1) can be rewritten in the following form

$$LCC = C_{cap\ PW} - C_{sav\ PW} - \sum_{k=1}^{K} S_{k\ PW} \quad (2)$$

where $C_{cap\ PW}$ is the PW of the total capital cost of the system over the project lifetime, $C_{sav\ PW}$ is the PW of the total system savings (or the difference between the PWs of the total system income and the total system outcome) arising from the total operational costs of the system over the project lifetime. Where,

$$C_{cap\ PW} = \sum_{k=1}^{K} \left(I_{k\ i} + R_{k\ PW} + OM_{k\ PW} \right) \quad (3)$$

And

$$C_{sav\ PW} = C_{EVs\ PW} \quad (4)$$

As Eq. (1) shows, there are PWs of some annual payments or revenues as well as of salvage values are needed. Thus, for a project lifetime of *N* years, a nominal interest rate r_n, and an nominal inflation rate *j* (induced by prices increases), the PWs of the different costs can be calculated as follows [28].

4.2 Calculation of PW of Salvage Value

If the salvage value of a component *k* at present is S_k (\$) (because it is reaching the end of its lifecycle), then it is expected that the salvage value of the component will be $S_k . (1+j)^N$ (i.e., N years from now, considering the component remains in service). Therefore, taking the interest rate into account, the PW of $S_k . (1+j)^N$, is [28]

$$S_{k\ PW} = S_k . \left(\frac{1+j}{1+r_n} \right)^N = S_k . fac_1 \quad (5)$$

4.3 Calculation of PW of Annual Payments or Revenues

If the current value of any annual payment (e.g., O&M) or revenue (e.g., cost of electrical energy) is α_{AP} (\$/yr), then at year x the value of the annual payment or revenue will be $\alpha_{AP} . (1+es)^x$ and having a PW of $\alpha_{AP} . \left(\frac{1+es}{1+r_n} \right)^x$ [28].

Where, *es* is the escalation rate, that is not necessarily equal to the general inflation rate.

Accordingly, the summation of the PWs of all the annual payments or revenues is calculated as follows

$$C_{AP\ PW} = \alpha_{AP} . \sum_{x=1}^{N} \left(\frac{1+es}{1+r_n} \right)^x = \alpha_{AP} . fac_2 \quad (6)$$

4.4 Levelized Cost of Energy

The *LCOE* is the average cost of the unit electricity (\$/kWh) that the investors of the renewable energy-based projects must sell their production of electrical energy to the consumers at prices not lower than its value to earn a profit [28-30]. The value of the *LCOE* can be calculated using as follows [14, 29-31]

$$LCOE = \frac{\left(C_{cap\ PW} - \sum_{k=1}^{K} S_{k\ PW} \right)}{E_{LT\_served}} \times CRF \quad (7)$$

where E_{LT_served} is the annual station total load served (kWh/yr), and CRF is the capital recovery factor, which can be calculated as [9]

$$CRF = \frac{r(1+r)^N}{(1+r)^N - 1} \quad (8)$$

where *r* denotes the real interest rate, which is given by [22]

$$r = \frac{r_n - j}{1+j} \quad (9)$$

4.5 Payback Period

The payback period is the parameter that determines the duration of time (yrs) that must elapse to recover the PW of the total capital cost of the system over the project lifetime (i.e., it is the time at which the total system cost will be zero) [32]. The shorter this period is, the more attractive the investment; since the project will be profitable after this period. This period can be estimated as [33]

$$T_{PB} = \frac{C_{cap\ PW}}{C_{ann\ sav\ PW}} \tag{10}$$

where $C_{ann\ sav\ PW}$ is the PW of the annual savings of the system, which can be given by

$$C_{ann\ sav\ PW} = C_{sav\ PW} \times CRF \tag{11}$$

5. Problem Formulation

The primary concern during the design of PV-battery stand-alone FCSEVs is estimating the size of each component of the system so that the station total load can be met economically and reliably. Thus, the formulated objective function can be as follows

1. minimizing the LCC of the system (i.e., $min.\ LCC$)
2. ensuring that the station annual total load (E_{LT}) is served according to certain reliability criteria

While minimizing the objective function LCC, the constraints must be met in such a way that certain reliability criteria are met while serving the station's annual total load. The $LPSP$ is used, here, to measure the system reliability, which is defined by the long-term average fraction of the total load that cannot be provided by the PV-battery stand-alone system.

A $LPSP$ of 1 indicates that the total load will never be satisfied, while a $LPSP$ of 0 indicates that the total load will always be satisfied. Therefore, the $LPSP$ constraint of the proposed system must be written in such a way that it remains lower than a certain preset value $LPSP^*$ during the considered time period of *T*. This constraint can now be expressed as follows

$$LPSP = \frac{\sum_{t=1}^{T} LPS(t)}{\sum_{t=1}^{T} E_{LT}(t)} \le LPSP^* \tag{12}$$

where *LPS*(*t*) represents the loss of power supply at any given hour *t*. It also refers to the deficit in total load energy caused when the available generated energy from the PV arrays and the energy stored in batteries does not meet the total load demand $E_{LT}(t)$ during the hour t. In addition, *T* denotes the operation time (in this work, *T* = 8760 hr).

6. LCC Estimation

6.1 The PV Array

For the case of the PV array, if the design variable is the total number of the PV modules (N_{PV}), then the total PW of the initial and replacement investments of the PV array is given by [28]

$$I_{PV} + R_{PV\,PW} = \alpha_{PV} . P_{module\_max} . N_{PV} = c_1 . N_{PV} \tag{13}$$

where α_{PV} is the initial cost of the used PV module ($/W$_P$), P_{module_max} is the rated power of the used PV module (295 Wp), and N_{PV} is the total number of PV modules. It is worth mentioning here that the PV array lifetime is equal to the project lifetime, thus the replacement cost of the PV array is negligible (*i.e.*, $R_{PV\,PW} = 0$).

Also, the total PW of the yearly O&M cost of the PV array would be

$$OM_{PV\ PW} = \alpha_{PV\ OM} . P_{module\_max} . N_{PV} . fac_2 = c_2 . N_{PV} \tag{14}$$

where $\alpha_{PV\ OM}$ is the PV module yearly O&M cost ($/W$_P$/yr).

In addition, the salvage value can be obtained by multiplying the total number of PV modules by the rated power of the utilized PV module and by the selling price per W$_P$, and the total PW of the salvage value of the PV array would be

$$S_{PV\ PW} = S_{PV} . P_{module\_max} . N_{PV} . fac_1 = c_3 . N_{PV} \tag{15}$$

6.2 The Battery Storage

Since the storage battery lifetime L_B is shorter than that of the PV modules, then it is needed to purchase additional storage batteries before the project lifetime comes to its end. Thus, the number of times, within *N* years, a battery storage is needed is $X_B = N / L_B$ (rounded to the greater integer) [28]. If α_B is the initial price of the battery unit in $/Wh, the total PW of the initial and replacement investments in batteries is as follows

$$I_B + R_{B\,PW} = \alpha_B . N_B . C_{sys\_unit} . \sum_{x=1}^{X_B} \left(\frac{1+es}{1+r_n} \right)^{(x-1).L_B} = c_4 . N_B \tag{16}$$

where N_B denotes the total number of the system battery units, C_{sys_unit} denotes the used nominal capacity of the system battery unit (Wh).

If the yearly O&M cost of one watt-hour of battery storage is $\alpha_{B\,OM}$ ($/Wh/yr), then the total yearly O&M cost of the battery storage would be $OM_B = \alpha_{B\,OM} . C_{sys\_unit} . N_B$, and the PW of all the yearly costs would be [28]

$$OM_{B\,PW} = \alpha_{B\,OM} . N_B . C_{sys\_unit} . fac_2 = c_5 . N_B \quad (17)$$

Noting, here, that the salvage value of the battery units is considered to be negligible $(i.e., S_{B\,PW} = 0)$.

6.3 The Utilized Converters

The cost of the bidirectional DC-DC converter that is used for charging and discharging the system battery storage is given by

$$C_{bi\_conv\_B} = \alpha_{bi\_conv\_B} . max(P_{ch\_\max}, (P_{disc\_\max} . \eta_{bi\_DC-DC})) = c_6 \quad (18)$$

where $\alpha_{bi\_conv\_B}$ denotes the cost of the utilized DC-DC converter in $/W, $P_{ch\_\max}$ denotes the maximum charging power of the system battery, $P_{disc\_\max}$ denotes the maximum discharging power of the system battery, and η_{bi_DC-DC} is the utilized converter efficiency. Also, the cost of the DC-DC converters that are used to charge the EVs is given by

$$C_{conv\_EV} = \alpha_{conv\_EV} . P_{EV\_ch} . N_{ch\_P} = c_7 \quad (19)$$

where α_{conv_EV} is the cost of the utilized converters in $/W and P_{EV_ch} is the rated power of the EV charger. In addition, the cost of the DC-AC converter that is used to power the station base load is given by

$$C_{inv} = \alpha_{inv} . P_{inv\_r} = c_8 \quad (20)$$

where α_{inv} is the cost of the utilized converter in $/W and P_{inv_r} is its rated power in Watt. It is worth mentioning here that the lifetimes of all the utilized converters are assumed to equal the project lifetime, i.e., the replacement costs of all the converters are negligible. Therefore, the PWs of all the converters costs are as indicated in Eqs. (18)-(20).

6.4 The Energy Sold to EVs

The PW of the cost of the electricity sold to EVs can be calculated as follows

$$C_{EVs\,PW} = \alpha_{EVs} . E_{EVs} . fac_2 = c_9 \quad (21)$$

where α_{EVs} denotes the unit electricity cost of the energy sold to the EVs ($/Wh) and E_{EVs} denotes the annual energy sold to the EVs (Wh/yr).

7. Mathematical Modeling of the Proposed System

7.1 The PV Array

The electrical output power of the PV array depends on the solar insolation and the cell temperature as given by [34-36]

$$P_{PV} = N_{PV} \times P_{\text{module\_max}} \times \left(\frac{G(t)}{G_{ref}} \right) \times \left[1 + K_t \left(T_c - T_{ref} \right) \right] \quad (22)$$

where $G(t)$ is the solar insolation in W/m^2, G_{ref} is the reference solar insolation of 1000 W/m^2, T_c denotes the cell temperature in ^{o}C, T_{ref} is the reference cell temperature of 25 °C, and K_t is the temperature coefficient of the utilized PV module.

7.2 Modeling of the System Battery

In the proposed FCSEVs, the battery storage can be charged or discharged to balance electricity supply and demand. The stored energy in battery storage at any time *t* can be given by [29]

$$E_B(t) = N_B \times C_{sys\_unit} \times \frac{SOC(t)}{SOC_{max}} \quad (23)$$

where $SOC(t)$ denotes the state of charge of the battery any time *t*, and SOC_{max} denotes the maximum state of charge of the battery. It is worth mentioning here that the used batteries, in this work, are lithium-ion batteries of 25.6 V, 200 Ah each.

The battery *SOC* can be estimated at any time, during the charging and discharging process, by using the following equation [28, 37].

$$SOC(t) = SOC(t-1) \times (1-\delta_B) - \frac{P_B(t) \times \eta_{sys\_B} \times \Delta t}{N_B \times C_{sys\_unit}} \quad (24)$$

where δ_B is the self-discharge rate of the battery storage, which is neglected in this work, Δt is the simulation step time (which is set, in this work, to equal 1 hr), η_{sys_B} is the charge efficiency of the system battery, and $P_B(t)$ is the battery charging/discharging power at any hour. Noting that during the charging process, the battery power P_B flows toward the battery (i.e., $P_B < 0$) and during the discharging process, the battery power flows outside the battery (i.e., $P_B > 0$).

To maintain the battery life, the battery should not be over-charged or over-discharged. Thus, the *SOC* of the battery at any given hour *t* must adhere to the following constraint [28]

$$SOC_{min} \le SOC\,(t) \le SOC_{max} \quad (25)$$

where SOC_{min} and SOC_{max} are the battery minimum and maximum permissible *SOC*, respectively.

7.3 Daily EVs Power Load Demand

The energy consumption of an EV depends on the travelled distance, the battery capacity, and the driving mode. Assuming that an EV is charged once a day, the daily average power demand of an EV (P_{EV_avg}) is the average power required to increase the *SOC* of the EV battery from its initial value (SOC_i) to its final value (SOC_f) over a daily charging period of time T_{ch} [38].

Consequently, the daily average maximum power demanded by a single EV battery in kW at the end of the given charging time T_{ch} can be given by

$$P_{EV\_avg} = \frac{C_{EV} \times DOD_{\max}}{T_{ch}} \quad (26)$$

where C_{EV} denotes the total nominal battery capacity of the EV in kWh, DOD_{max} denotes the maximum permissible depth of discharge of the EV battery, and T_{ch} denotes the daily charging time of the EV battery in hours. In this work, T_{ch} is set to equal half hour (i.e., to achieve the desired fast charging principle for the EV battery) and DOD_{max} to 70% [38].

Thus, the daily average maximum power demanded by a number of EVs will be estimated as a function of time as follows

$$P_{EVs\_avg}(t) = \frac{N_{ch\_P} \times C_{EV} \times DOD_{max} \times D(t)}{T_{ch}} \quad (27)$$

where N_{ch_P} is the number of the charging points in the station and $D(t)$ is the daily time-dependent duty cycle of the station.

8. Energy Management and System Reliability

Firstly, it is assumed, in this work, that the utilized DC-DC converter for the MPPT and the distribution lines are ideal (i.e., they are lossless). Whereas, on the other hand, all the remaining DC-DC converters in this work, whether they are unidirectional or bidirectional, can be excluded from this assumption and are assumed to have equal and constant efficiencies (i.e., $\eta_{bi\_DC-DC} = \eta_{uni\_DC-DC} = \eta_{DC-DC}$). Also, it is assumed, in this work, that the utilized DC-AC converter has constant efficiency equaling to η_{DC-AC}. In addition, it is assumed that both the charge efficiency of the system battery (η_{sys_B}) and that of the EV battery (η_{EV_B}) are, respectively, set to equal to their corresponding manufacturers' round-trip efficiencies, and their discharging efficiencies are set to be 100%.

Figure 5 illustrates the designed energy management strategy for the proposed PV-battery stand-alone FCSEVs. The primary goals of this strategy are to manage the energy flow within the considered system to serve the station total load reliably and to safely charge and discharge the system battery.

In this work, the only generated power of the proposed system at any hour *t* is the PV array output power (i.e., $P_{PV}(t)$), whereas the storage system battery is used as a backup for this system. Therefore, the desired station total load demand at any given hour *t* may or may not be met based on the corresponding values of the generated PV power and the available battery $SOC(t)$ at that hour.

The desired station total load demand referred to the DC bus can be estimated at any hour t from

$$P_L^*(t) = \frac{P_{EVs\_avg}(t)}{\eta_{EV\_charging}} + \frac{P_{base\_load}(t)}{\eta_{DC-AC}} \quad (28)$$

where $P_{EVs\_avg}(t)$ is the hourly average maximum power demand of the EVs, $P_{base\_load}(t)$ is the hourly average base load demand of the station, $\eta_{EV\_charging}$ is the total efficiency of the EVs charging path, which is given by the result of multiplying the efficiency of the DC-DC converter by that of a single EV battery (i.e., $\eta_{DC-DC} \times \eta_{EV\_B}$).

The proposed energy management strategy of the PV-battery stand-alone FCSEVs can be summarized in the following points:

- If $(P_{PV}(t) > P_L^*(t))$ and $(SOC(t-1) < SOC_{max})$, then satisfy the station total load and charge the system battery using Eq. (24) with the excess PV output power of Eq. (29).

$$P_B(t) = [P_L^*(t) - P_{PV}(t)]\,\eta_{DC-DC} \tag{29}$$

Afterwards, check if $(SOC(t) \geq SOC_{max})$, then stop system battery charging, set $SOC(t) = SOC_{max}$, and dump the surplus PV output power estimated by

$$P_{dump}(t) = P_{PV}(t) - [P_L^*(t) + (\frac{N_B \times C_{sys\_unit}}{\eta_{DC-DC} \times \eta_{sys\_B} \times \Delta t} \times (SOC_{max} - SOC(t\text{-}1)))] \tag{30}$$

- If $(P_{PV}(t) > P_L^*(t))$ and $(SOC(t-1) \geq SOC_{max})$, then satisfy the station total load, stop charging of the system battery, set $SOC(t) = SOC_{max}$, and dump the surplus PV output power estimated by

$$P_{dump}(t) = P_{PV}(t) - P_L^*(t) \tag{31}$$

- If $(P_{PV}(t) = P_L^*(t))$, then satisfy the station total load only.
- If $(P_{PV}(t) < P_L^*(t))$ and $(SOC(t-1) > SOC_{min})$, then satisfy the station total load by discharging the system battery using Eq. (24) to cover the deficit in the station total load power. The discharging power of the system battery in this case will be estimated from

$$P_B(t) = [P_L^*(t) - P_{PV}(t)] / \eta_{DC-DC} \tag{32}$$

Afterwards, if $(SOC(t) \leq SOC_{min})$, then stop discharging of the system battery, set $SOC(t) = SOC_{min}$, and estimate the deficit in the station total load power referred to the DC bus from

$$P_{deficit}(t) = P_L^*(t) - [P_{PV}(t) + (\frac{N_B \times C_{sys\_unit} \times \eta_{DC-DC}}{\Delta t} \times (SOC(t-1) - SOC_{min}))] \tag{33}$$

- If $(P_{PV}(t) < P_L^*(t))$ and $(SOC(t-1) \leq SOC_{min})$, then stop discharging of the system battery, set $SOC(t) = SOC_{min}$, and calculate the deficit in the station total load power referred to the DC bus using Eq. (34).

$$P_{deficit}(t) = [P_L^*(t) - P_{PV}(t)] \tag{34}$$

According to the previous assumptions mentioned in this work, which were the simulation step time Δt was set to equal 1 hr and all the considered system powers during Δt were constants, then any considered power of the system will numerically equal to its corresponding energy within Δt

The *LPSP* constraint of Eq. (35), which is a non-linear constraint of the variables N_{PV} and N_B, can now be formulated as follows

$$LPSP = \frac{\sum_{t=1}^{T} P_{deficit}(t) \times \Delta t}{\sum_{t=1}^{T} P_L^*(t) \times \Delta t} \tag{35}$$

The program that calculates the *LPSP* of the proposed PV-battery stand-alone system was written in MATLAB code in an M-file. The flowchart of the designed energy management is indicated in Fig. 5. The hourly average global solar insolation data (G) over one typical year, the hourly average maximum power demand of the EVs (P_{EVs_avg}) over one typical year, and the hourly average base load demand of the station (P_{base_load}) over one typical year are the input data for this program.

The sizes of the system components must be, also, adhered to the following two additional bounds, that are

$$0 \leq N_{PV} \leq N_{PV\_max} \tag{36}$$

and

$$0 \leq N_B \leq N_{B\_max} \tag{37}$$

The maximum number of PV modules (N_{PV_max}) is originally restricted by the maximum available area for the PV

array, and it may be additionally restricted according to the preallocated budget of the PV modules. At the same time, the maximum number of units of the system battery (N_{B_max}) (which can be calculated from Eq. (38)) is mainly restricted by the largest number of continuous cloudy days of the considered site ($N_{c\ max}$), and it may be additionally restricted as well according to the preallocated budget of the system battery.

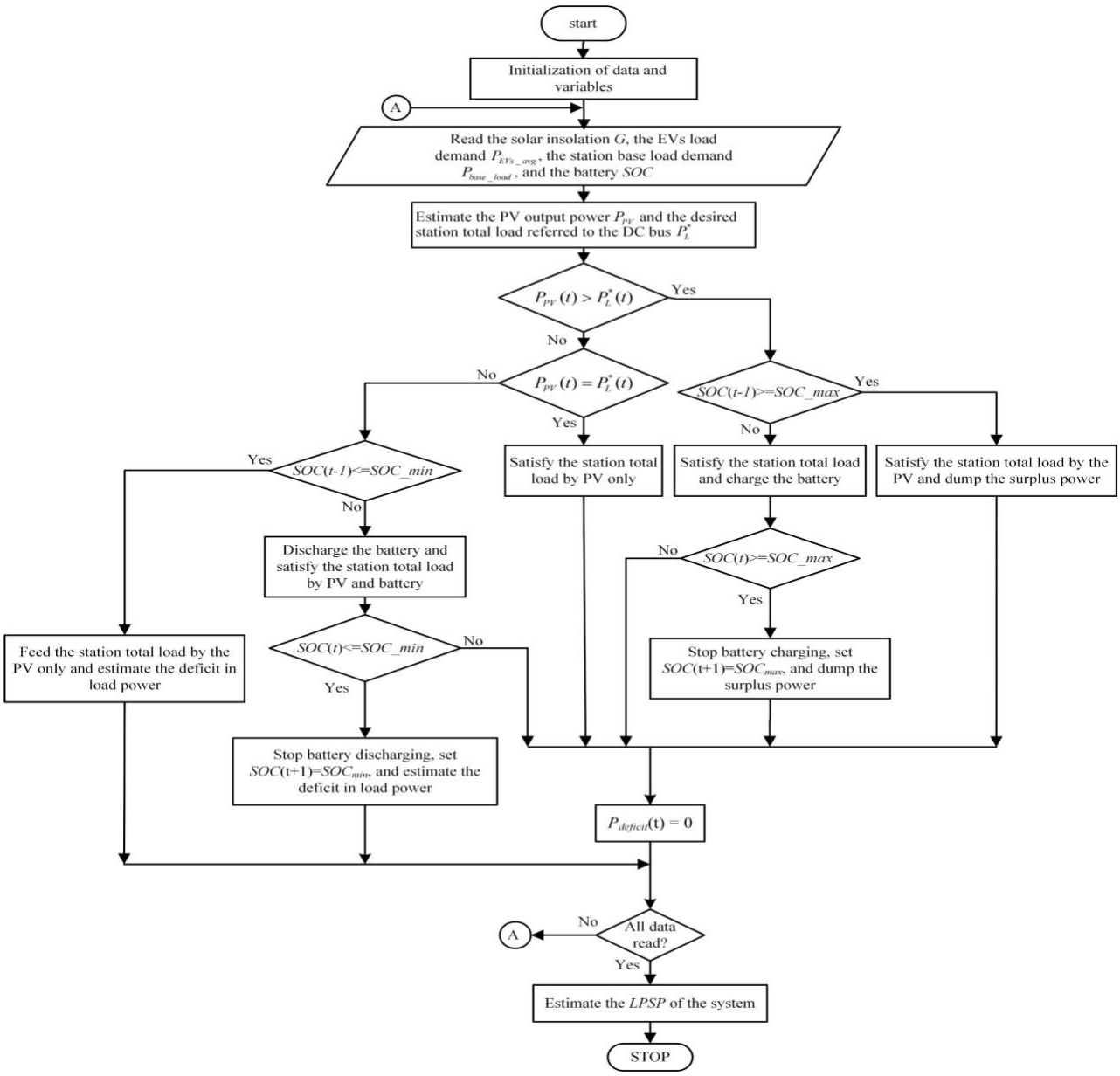

Fig. 5. Proposed energy management of the PV-battery stand-alone FCSEVs.

$$N_{B\_\max} = \frac{N_{c\ max}\left(E_{EVs\_daily} + E_{base\ daily}\right)}{C_{sys\_unit} \times DOD_{\max} \times \eta_{DC-DC}} \tag{38}$$

Where, E_{EVs_daily} is the daily average maximum energy demanded by the EVs (Wh/day) and $E_{base\ daily}$ is the daily average base load energy demand of the station (Wh/day). Noting, here, that the $N_{c\ max}$ for the considered location is about two days.

9. Final Form and Snake Optimization

It is now possible to rewrite the optimization problem in its final form as follows

1. Minimize the cost function (also called objective function or fitness function) $f = LCC$

$$(c_1 + c_2 - c_3).N_{PV} + (c_4 + c_5).N_B + c_6 + c_7 + c_8 - c_9 \quad (39)$$

2. Subject to

$$\left.\begin{array}{l} LPSP \le LPSP^* \\ 0 \le N_{PV} \le N_{PV\_max} \\ 0 \le N_B \le N_{B\_\max} \end{array}\right\} \quad (40)$$

To solve the previous final form of the optimization problem, snake optimizer (SO) is utilized. This optimizer, which was developed by [39], is inspired by the snakes' mating behaviour. If there is an abundance of food and a low ambient temperature, snakes often fight to get the best partners. Otherwise, the snakes will only search for food or eat the exiting food. Therefore, the search process of the SO is based on two phases, which are exploration and exploitation.

The flowchart of the SO is shown in Fig. 6 [39]. It starts by generating a uniformly distributed random population. The initial population can be obtained from

$$X_i = X_{min} + rand \times (X_{max} - X_{min}), \quad i \in \{1, 2, ..., N_{Pop}\} \quad (41)$$

where X_i refers to the individual at position *i* of the initially generated population for the optimization problem (this individual is actually a vector whose length equals the number of the independent variables of the problem), N_{Pop} is the total number of the population individuals or may also called the problem swarm, *rand* is a uniformly distributed random number generated in the range between 0 and 1, and $X_{\min}$ and $X_{\max}$ denote the individuals lower and upper bounds of the problem variables, respectively.

Afterwards, the problem swarm is divided equally into two groups: males and females, as

$$N_m \approx \frac{N_{Pop}}{2} \quad (42)$$

$$N_f = N_{Pop} - N_m \quad (43)$$

where N_m and N_f are the numbers of individuals in the male and female groups, respectively.

The next step is to find the best individual in each group, i.e., to get the best male and best female individuals that correspond to the best or minimum objective function (f_{m_best} and f_{f_best}) in each of the male and female groups, respectively. Afterwards, the ambient temperature ($Temp$) and the quantity of food (Q), in the current iteration ($Iter$), can be computed, respectively, from

$$Temp = exp\left(\frac{-Iter}{Iter_{max}}\right) \quad (44)$$

$$Q = 0.5 \times exp\left(\frac{Iter - Iter_{max}}{Iter_{max}}\right) \quad (45)$$

where $Iter_{max}$ refers to the maximum number of iterations.

The common behaviour of snakes is to check for the available quantity of food (*Q*) at first. If the value of *Q* is found to be lower than or equal a certain threshold value (i.e., $Q \le 0.25$), then the male and female snakes will search for food by updating the positions of their individuals randomly with respect to the food. This updating process is called the exploration phase and depends on the abilities of the individuals of each of the males and females to find food. The male and female abilities to find food can be found, respectively, from

$$A_{m\_i} = exp\left(\frac{-f_{m\_rand}}{f_{m\_i}}\right) \quad (46)$$

$$A_{f\_i} = exp\left(\frac{-f_{f\_rand}}{f_{f\_i}}\right) \quad (47)$$

where f_{m_rand} is the fitness of the random male individual (X_{m_rand}), f_{m_i} is the fitness of the i th individual in the male group (X_{m_i}), f_{f_rand} is the fitness of the random female individual (X_{f_rand}), and f_{f_i} is the fitness of the *i*th individual in the female group (X_{f_i}).

The randomly updated male and female individuals of position *i*, after carrying out this exploration phase, become

$$X_{m\_i}(Iter+1) = X_{m\_rand}(Iter) + Flag \times g \times A_{m\_i} \times ((X_{\max} - X_{\min}) \times rand + X_{\min}) \quad (48)$$

$$X_{f\_i}(Iter+1) = X_{f\_rand}(Iter) + Flag \times g \times A_{f\_i} \times ((X_{\max} - X_{\min}) \times rand + X_{\min}) \quad (49)$$

where X_{m_rand} and X_{f_rand} denote the male and female individuals of random positions, respectively, $rand$ is a random number between 0 and 1, g is a constant (=0.05), and $Flag$ is called the flag direction operator or diversity factor which is set randomly to either positive sign or negative sign; so as to increase the possibility of scanning all the possible directions in the given search space.

Whereas, on the other hand, if the food is available (i.e., $Q > 0.25$), then this phase is called the exploitation phase, which includes many transition phases that lead to many updates for the individuals of the two groups. These many updates will increase the opportunity of the SO to converge to the optimum solution of the optimization problem instead of diverging from it. If, in this phase, the ambient temperature ($Temp$) is hot (i.e., $Temp > 0.6$), then the snakes will only focus on eating the available food. Consequently, the male and female snakes will move to food, depending on the ambient temperature, by updating the positions of their individuals randomly with respect to the available food.

The randomly updated male and female individuals of position i, after carrying out this process, can be given by

$$X_{m\_i}(Iter+1) = X_{food}(Iter) + Flag \times g_1 \times Temp \times rand \times (X_{food} - X_{m\_i}(Iter)) \quad (50)$$

$$X_{f\_i}(Iter+1) = X_{food}(Iter) + Flag \times g_1 \times Temp \times rand \times (X_{food} - X_{f\_i}(Iter)) \quad (51)$$

where X_{food} is the best individual of the two groups with respect to the available food, and g_1 is constant (= 2).

In addition, in this phase (i.e., $Q > 0.25$), if the ambient temperature ($Temp$) is cold (i.e., $Temp \le 0.6$), then the snakes will randomly decide to be either in fighting mode or mating mode. In the fighting mode, the snakes (male and female) individuals will update their positions randomly depending on the fighting abilities of individuals, the available food quantity, and the best individual in the other group.

The fighting abilities of the individuals in the male and female groups are given, respectively, by

$$F_{m\_i} = exp\left(\frac{-f_{f\_best}}{f_{m\_i}}\right) \quad (52)$$

$$F_{f\_i} = exp\left(\frac{-f_{m\_best}}{f_{f\_i}}\right) \quad (53)$$

where f_{f_best} and f_{m_best} are the fitness of the best individual in female and male groups, respectively.

The updated individuals of position i in the male and female groups, after fighting, can be given, respectively, by

$$X_{m\_i}(Iter+1) = X_{m\_i}(Iter) + g_1 \times F_{m\_i} \times rand \times (Q \times X_{f\_best} - X_{m\_i}(Iter)) \quad (54)$$

$$X_{f\_i}(Iter+1) = X_{f\_i}(Iter) + g_1 \times F_{f\_i} \times rand \times (Q \times X_{m\_best} - X_{f\_i}(Iter)) \quad (55)$$

where X_{f_best} and X_{m_best} are the best individual in the female group and male groups, respectively.

Whereas, in the mating mode, the snakes (males and females) individuals will update their positions randomly depending on the mating abilities of individuals, the available food quantity, and the corresponding individual in the other group.

The mating abilities of the individuals in the male and female groups are given, respectively, by

$$M_{m\_i} = exp\left(\frac{-f_{f\_i}}{f_{m\_i}}\right) \quad (56)$$

$$M_{f\_i} = exp\left(\frac{-f_{m\_i}}{f_{f\_i}}\right) \quad (57)$$

The updated individuals of position i in the male and female groups, after mating, can be given, respectively, by

$$X_{m\_i}(Iter+1) = X_{m\_i}(Iter) + g_1 \times M_{m\_i} \times rand \times (Q \times X_{f\_i}(Iter) - X_{m\_i}(Iter)) \quad (58)$$

$$X_{f\_i}(Iter+1) = X_{f\_i}(Iter) + g_1 \times M_{f\_i} \times rand \times Q \times X_{m\_i}(Iter) - X_{f\_i}(Iter)) \quad (59)$$

After carrying out the mating process, the females lay eggs, which may randomly hatch or not hatch. If the eggs

do not hatch, the current individuals in the male and female groups are kept without change. On the other hand, if the eggs have hatched, the worst individual from each of the male and female groups will be replaced as follows

$$X_{m\_worst}(Iter+1) = X_{min} + rand \times (X_{max} - X_{min}) \quad (60)$$

$$X_{f\_worst}(Iter+1) = X_{min} + rand \times (X_{max} - X_{min}) \quad (61)$$

where X_{m_worst} and X_{f_worst} are the worst individuals in the male and female groups, respectively.

Finally, all the current individuals in each of the male and female groups, which resulted from carrying out any one of the previous updates in the current iteration, must be checked and set to be within their upper and lower bounds (i.e., X_{max} and X_{min}). After ensuring that all the final individuals of the current iteration are within their upper and lower bounds, they are utilized to constitute the initial population for the next iteration. All the previous processes will be repeated until the executed number of iterations equals the preset maximum limit (i.e., $Iter_{max}$).

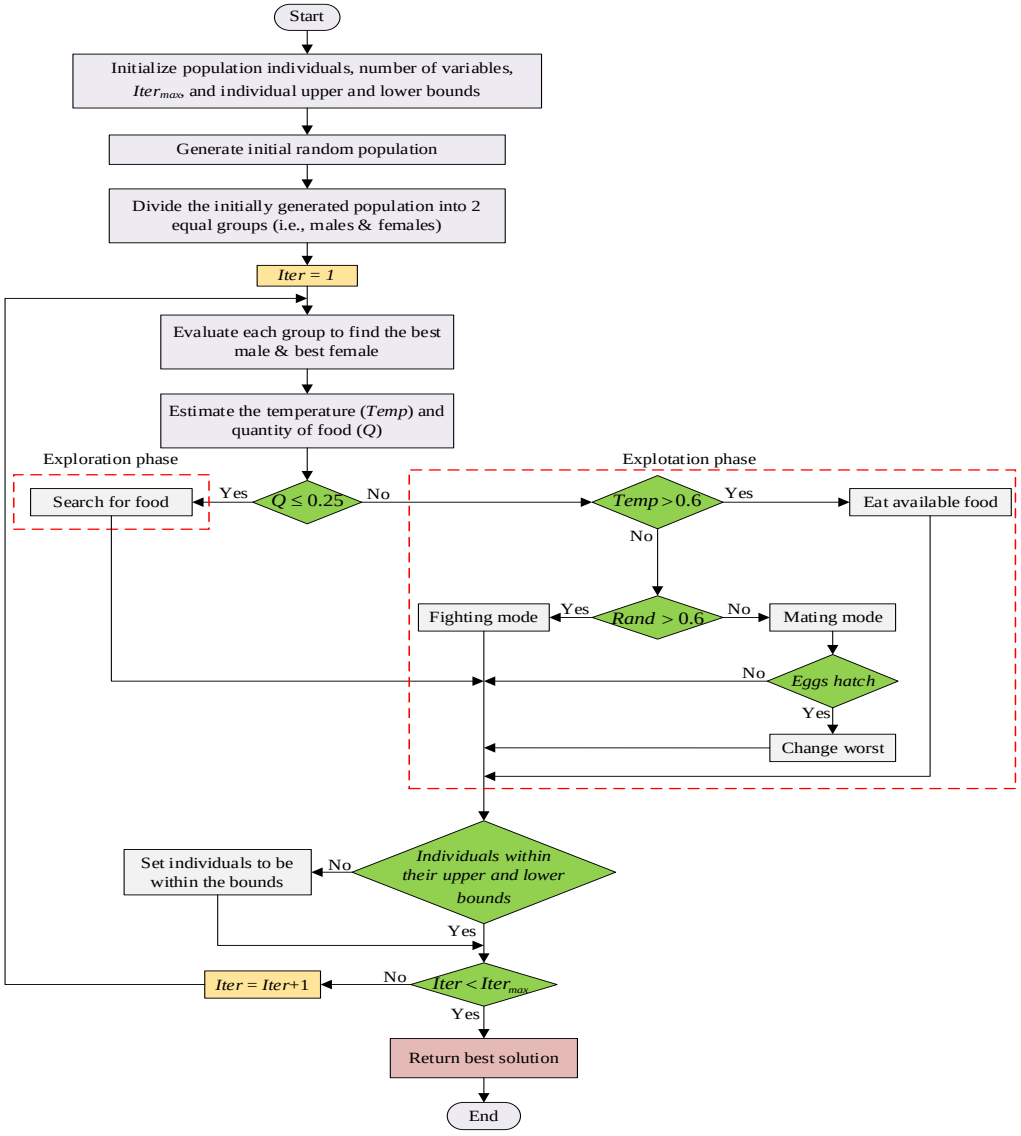

Fig. 6. Flowchart of SO.

10. Simulation Results and Economic Analysis

The formulated optimization problem of the considered PV-battery stand-alone FCSEVs is solved, in this work, by using the SO. The code of this SO was designed by using MATLAB software. The individual of the considered optimization problem, in this work, contains two variables, which are N_{PV} and N_B. Also, the used population size and the maximum number of iterations are set to 50 and 200, respectively.

The utilized different techno-economic parameters of the proposed PV-battery stand-alone FCSEVs are given in Table 1. This table shows that the lifetime of the storage battery is 10 yrs. Therefore, the system battery must be replaced twice before the project comes to its end. It is to be noted, here, that the shown values of the interest, inflation, and escalation rates are for Egypt during Jan 2022 [32, 40, 41].

Table 1. The techno-economic parameters of the proposed PV-battery stand-alone FCSEVs.

Parameter	Value
Initial capital cost of PV module ($/kW)	550
O&M cost of PV ($/yr)	10
Salvage value of PV ($/kW)	5
PV lifetime (yrs)	25
Initial capital cost of storage battery ($/kWh)	300
O&M cost of storage battery ($/yr)	2.75
SOC_{min}	0.3
SOC_{max}	0.9
Round-trip efficiency of system battery (%)	98
Storage battery lifetime (yrs)	10
Initial capital cost of DC-DC converters ($/kW)	100
Initial capital cost of DC-AC converter ($/kW)	100
Efficiency of all converters (%)	96
Lifetime of converters (yrs)	25
Nominal interest rate (%)	8.25
Nominal inflation rate (%)	7.3
Escalation rate (%)	7

The resulted SO-based optimum sizes of the components of the PV-battery stand-alone system are found to be $N_{PV} = 4068$ and $N_B = 497.1$ The corresponding fitness function optimization (i.e., minimization of the considered objective function, which equals the *LCC* of the system) along the successive iterations of the SO is shown in Fig. 7, which indicates that the system is optimized after just thirteen iterations only, i.e., the SO has high convergence capability.

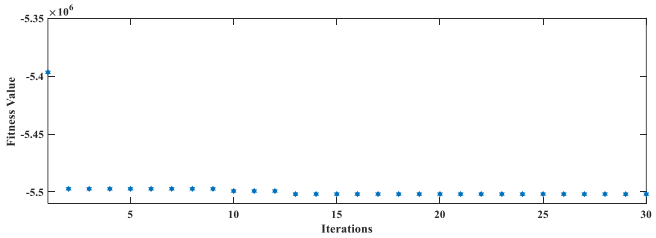

Fig. 7. Optimization of the fitness function using SO.

Table 2 illustrates the SO-based optimum and selected ratings and the corresponding initial capital costs of all components included in the PV-battery stand-alone FCSEVs. This table indicates that the optimal ratings of the PV and the storage battery are 1200.06 kWp and 2545.152 kWh, respectively. The shown optimum rating of the battery storage can satisfy the daily load for 7.61 hrs, i.e., it can provide 7.61 autonomy hours per day. It is shown that the designed optimum rating of the DC-DC converter of the EVs is 70.98 kW. However, it is well-known that the available higher standard rating of this converter is 100 kW [4, 42], thus the standard converter was selected to be used in this work, as indicated in Table 2.

Also, it is worth mentioning that the series configurations of the PV array and the storage battery can be decided according to the desired value of the system DC bus voltage and the selected suitable duty cycle of the corresponding DC-DC converter, whereas the corresponding parallel configurations can be decided according to the total number of the PV modules and battery units and their corresponding selected series configurations.

In order to evaluate the robustness of the utilized SO in optimizing the formulated optimization problem of the considered PV-battery stand-alone FCSEVs, the SO algorithm should be compared to other common optimization algorithms, e.g., grey wolf optimization (GWO), particle swarm optimization (PSO), genetic algorithm (GA), ant colony optimization (ACO), etc. In this work, the utilized SO algorithm is compared with three common well-known algorithms: GWO, PSO, and GA.

For a desired $LPSP^* = 0.02$, Table 3 shows a comparison among the resulted different optimum key parameters of the considered optimization problem by using the considered different optimization algorithms. These results include the optimized number of PV modules (N_{PV}), optimized number of system storage battery units (N_B), the PW of the total capital cost of the system ($C_{cap\ PW}$), the PW of the net profit

Table 2. Optimum and selected ratings and initial capital costs of all system components.

Item	Component rating & cost	PV array	Storage battery	Bidirectional DC-DC converter of the storage battery	DC-DC converter(s) of EVs (5 units)	DC-AC converter
Optimal	Rating	1200.06 kWp	2545.152 kWh	668.09 kW	5× 70.98 kW	600 W
	Cost	660033 $ (Including cost of MPPT)	763545 $	66809 $	35490 $	60 $
Selected	Rating	1200.06 kW (N_{PV} = 4068, N_{PVs}=12, N_{PVp}=339, P_{max} =295W)	2549.76 kWh (N_B = 496, N_{Bs}=16, N_{Bp} = 31, C_{sys_unit} = 5.12 kWh)	700 kW	5× 100 kW	700 W
	Cost	660033 $ (Including cost of MPPT)	761856 $	70000 $	50000 $	70 $

Table 3. Comparison among different optimum key parameters of the optimization problem using different optimization algorithms.

Algorithm	No. of PV modules	No. of battery units	PW of total capital cost (× 10^6 $)	PW of net profit (× 10^6 $)	*LCOE* (¢/kWh)	T_{PB} (yr)
SO	4068	497.1	3.2209	5.5022	8.19	8.2528
GWO	4087.05	496.058	3.2210	5.50199	8.19	8.2531
PSO	4000	501	3.2212	5.5018	8.19	8.2535
GA	3945	504.3	3.2224	5.5002	8.20	8.2568

of the system at the end of the project lifetime, the levelized cost of energy (*LCOE*), and the payback period (T_{PB}). It is indicated, from this table, that the utilized SO algorithm gives the best optimization results compared to the other optimization algorithms, where it gives the lowest total capital cost, the highest net profit, the lowest *LCOE*, and the lowest payback period (T_{PB}).

Table 4 illustrates the yearly energetic results of the designed (i.e., selected) system. It should be noted, during the derivation of this table, that two essential conditions have to be satisfied to adopt and ensure the validity of the results included in this table:

1. The energy balance principle has to be satisfied at the DC bus, i.e., the sum of the generated PV energy and the energy discharged from the battery at the DC bus has to equal the sum of the station total load consumption and the excess PV energy.
2. The excess PV energy has to equal the sum of the battery charged energy at the DC bus and the dumped energy.

This table shows that the total generated PV energy throughout a year is 2794.6 MWh/yr. Also, the yearly excess PV energy is 1490.4 MWh/yr with a percentage of 53.33 % relative to the yearly generated PV energy, whereas the yearly unmet load is 36.274 MWh/yr with a percentage of 2.02 % relative to the yearly desired station total load consumption of 1793.4 MWh/yr. It is to be noted that the shown excess PV energy can be either stored in the battery storage or dissipated in the dump load; depending on the designed optimal energy management strategy. In addition, this table shows that the battery charged and discharged energy per year are 480.32 MWh/yr and 471.82 MWh/yr, respectively. Thus, for the used bidirectional DC-DC converter of the system storage battery having an efficiency of 96%, the corresponding values of these energies at the DC bus will become 500.33 MWh/yr and 452.95 MWh/yr, respectively.

Figure 8 shows the generated PV output power of the designed PV-battery stand-alone FCSEVs for every hour during the year. Also, Figs. 9 and 10 show the corresponding storage battery power and *SOC*, respectively.

Table 4. Yearly energetic results of the designed system.

Generated PV energy (MWh/yr)	Station total load consumption (MWh/yr)	Excess PV energy (MWh/yr)	Storage battery charged energy (MWh/yr)	Storage battery discharged energy (MWh/yr)	Dumped energy (MWh/yr)	Unmet load (MWh/yr)
2794.6	1757.2	1490.4	480.32	471.82	990.05	36.274

Therefore, Fig. 8 shows that the PV output power varies in direct proportion to the incident solar insolation. Whereas, Figs. 9 shows that the system battery is in charging or discharging mode depending on the generated PV power, the desired station total load demand, and on the battery *SOC*. Noting, here, that the values of the battery power are preadjusted to be positive during discharging and negative during charging, which is indicated in Fig. 9. In addition, Fig. 10 shows that the system storage battery is charged and discharged safely, because the battery *SOC* always stays within the preset designed minimum and maximum values of 0.3 and 0.9, respectively.

The excess PV power, the dumped power, and the deficit in the station total load power are shown in Figs. 11, 12, and 13, respectively. It is indicated from these figures that due to the long daylight hours during summer months and the corresponding high solar insolation intensity, there will be an excess in the generated PV power, which leads to a corresponding excess in the dumped power during these months, as shown in Figs. 11 and 12, respectively. Whereas, on the other hand, during the winter months, there will be short daylight hours and low solar insolation intensity. Thus, the generated PV power during these months will be lower than that of the summer months, which leads to a corresponding deficit in the station load power, as shown in Fig. 13.

Figure 14 illustrates the station total load served by the PV-battery stand-alone FCSEVs. Thus, this figure indicates that the load is fully satisfied during the summer months while it is partially satisfied during the winter months, as explained previously.

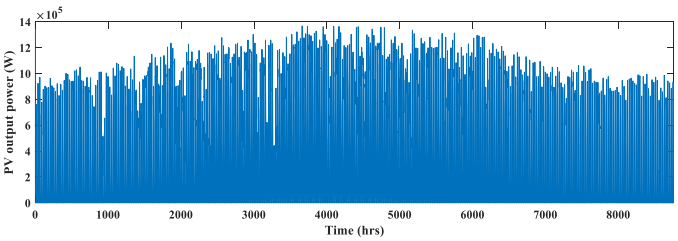

Fig. 8. Generated PV output power.

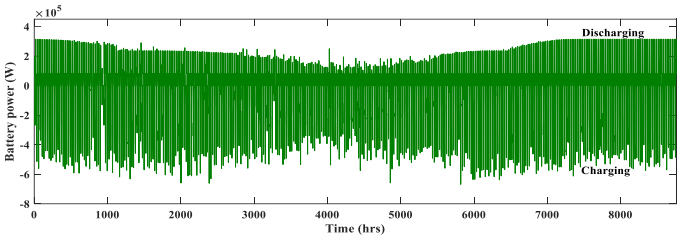

Fig. 9. Storage battery power.

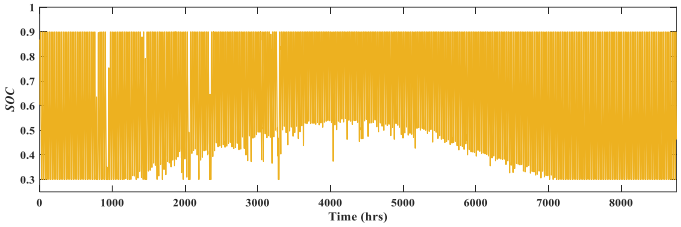

Fig. 10. SOC of the system battery.

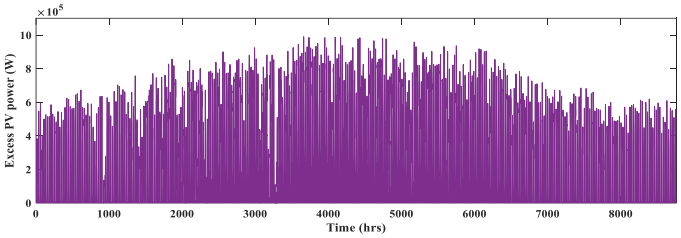

Fig. 11. Excess PV power.

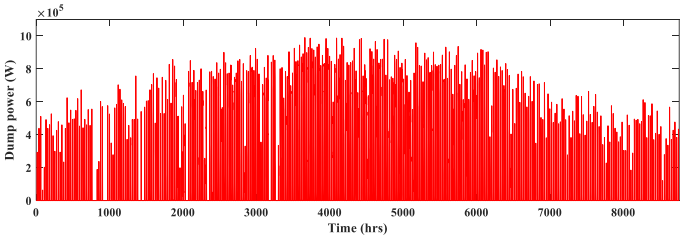

Fig. 12. Dumped power.

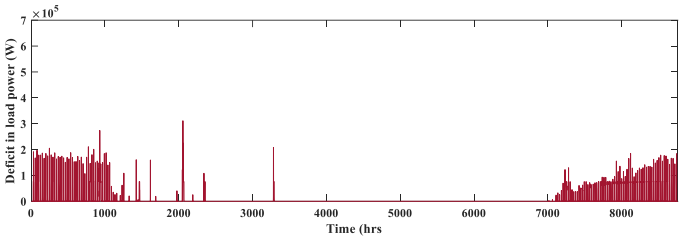

Fig. 13. Deficit in station total load power.

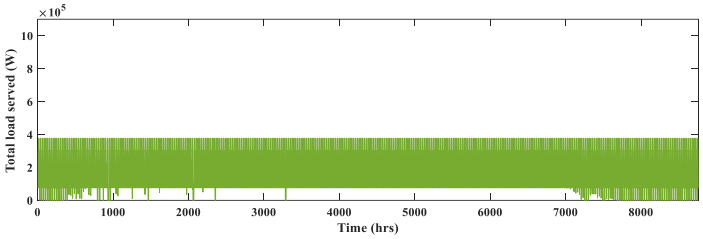

Fig. 14. Station total load served.

The PWs of the accumulated annual cash flow of the designed PV-battery stand-alone FCSEVs over the project lifetime is shown in Fig. 15. This figure indicates that the PW of the accumulated annual total capital cost will be linearly increased due to the accumulation of the incurred annual O&M costs and has two upward steps due to the accumulation of the replacement costs of the utilized system storage battery. The final value of the PW of the accumulated annual total capital cost at the end of the project lifetime is called the PW of the total capital cost, which is the main required cost to establish the designed PV-battery stand-alone FCSEVs.

Also, this figure indicates that the PW of the accumulated annual saving of the system (which is the difference between the PW of the accumulated annual income minus the PW of the accumulated annual outcome) varies linearly downwards and has negative values, since there is no outcome from the designed system and also since the values of the annual income of the system (which is the annual income of the electrical energy sold to EVs) are fixed over all years. Thus, the PW of the accumulated annual saving of the system is shown to be linearly decreasing downwards and having a negative slope as shown in Fig. 15. Noting, here, that the value of this slope equals the value of the annual saving of the system.

At the same time, this figure indicates that the accumulated annual total system cost (which is the algebraic sum of the PW of the total capital cost of the system and the PW of the accumulated annual saving of the system) is shown to be decreasing linearly from positive values to negative values with a slope equals the PW of the annual total system cost. Noting, here, that the final value at this line (i.e., at the end of the project lifetime) is called the PW of the net profit of the project, as shown in Fig. 15.

Finally, Table 5 illustrates the main economic parameters of the designed PV-battery stand-alone FCSEVs that can be used to decide the financial impact and profitability of the project. It is shown that the designed PV-battery stand-alone FCSEVs has slightly lower values of the main economic parameters compared to the optimal PV-battery stand-alone FCSEVs of Table 3, except for the value of the PW of the net profit; due to using nearly one unit of storage battery lower than the optimal PV-battery stand-alone FCSEVs, which leads to a corresponding reduction in the battery O&M and replacement costs.

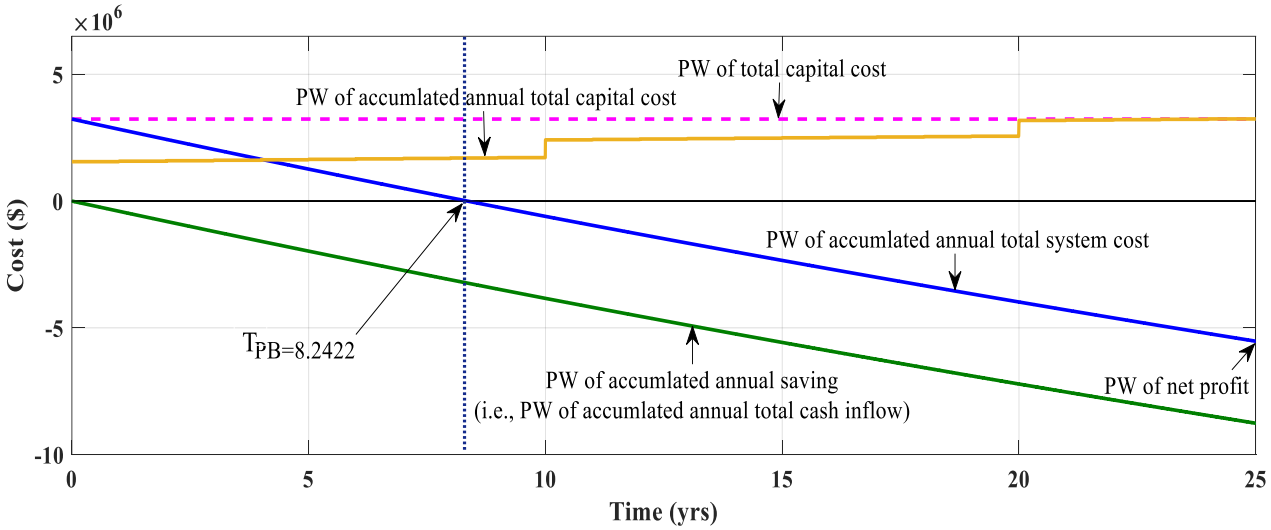

Fig. 15. Accumulated cash flow of the designed PV-battery stand-alone FCSEVs over the project lifetime.

Table 5. Main economic parameters of the designed PV-battery stand-alone FCSEVs.

PW of total capital cost ($\times 10^6$ \$)	PW of net profit ($\times 10^6$ \$)	*LCOE* (¢/kWh)	T_{PB} (yrs)
3.2160	5.5049	8.18	8.2422

11. Conclusions

In this paper, an optimization problem for sizing a proposed PV-battery stand-alone FCSEVs has been presented. The considered optimization problem has been formulated, in this work, to achieve a minimum total cost for the proposed system and to guarantee high reliability for the station total load. The reliability of the proposed system has been estimated in terms of the *LPSP* of the system during one typical year. The energy management strategy has been designed to optimally manage the energy flow within the considered system; so as to serve the station total load reliably and to safely charge and discharge the system battery.

A recent optimization algorithm, known as SO, has been utilized to solve the formulated optimization problem by using MATLAB software. The yielded results have indicated that the SO converges very well and it is feasible for sizing the proposed system. Also, the yielded results have indicated that the SO is more robust in satisfying the desired ultimate goals of the considered optimization problem compared to other common meta-heuristic algorithms. In addition, the economic viability of the designed PV-battery stand-alone FCSEVs has been decided based on carrying out a techno-economical study for the considered system. Finally, it can be concluded that the investment in establishing PV-battery stand-alone fast charging stations for electric vehicles is encouraging and profitable. Thus, the Egyptian government should encourage and promote the establishment of such charging stations, especially along the highways that are far away from the utility grid.

References

[1] J. Ugirumurera and Z. Haas, "Optimal Capacity Sizing for Completely Green Charging Systems for Electric Vehicles," IEEE Transactions on Transportation Electrification, vol. 3, no. 3, pp. 565-577, 2017.

[2] M. AKIL, E. Dokur, and R. Bayindir, "A Coordinated EV Charging Scheduling Containing PV System," International Journal of Smart Grid-ijSmartGrid, vol. 6, no. 3, pp. 65-71, 2022.

[3] M. Akil, E. Dokur, and R. Bayindir, "Impact of Electric Vehicle Charging Profiles in Data-Driven Framework on Distribution Network," in 9th International Conference on Smart Grid (ICSMARTGRID), IEEE, pp. 220-225, 2021.

[4] M. Brenna, F. Foiadelli, C. Leone, and M. Longo, "Electric Vehicles Charging Technology Review and Optimal Size Estimation," Journal of Electrical Engineering Technology, pp. 1-14, 2020.

[5] "Global EV Data Explorer. Available: https://www.iea.org/articles/global-ev-data-explorer."

[6] "The Global Electric Vehicle Market Overview In 2022: Statistics & Forecasts. Available: https://www.virta.global/global-electric-vehicle-market."

[7] S. Mohseni, S. Moghaddas-Tafreshi, and society, "A Multi-Agent System for Optimal Sizing of A Cooperative Self-Sustainable Multi-Carrier Microgrid," Sustainable cities, vol. 38, pp. 452-465, 2018.

[8] I. Hamdan, A. Maghraby, and O. Noureldeen, "Random Search Optimization Algorithm Based Control of Supercapacitor Integrated with Solar Photovoltaic System Under Climate Conditions," International Journal of Renewable Energy Research, vol. 12, no. 2, pp. 611-622, 2022.

[9] J. Vishnupriyan, D. Arumugam, N. M. Kumar, S. Chopra, and P. Partheeban, "Multi-Criteria Decision Analysis for Optimal Planning of Desalination Plant Feasibility in Different Urban Cities in India," Journal of Cleaner Production, vol. 315, p. 128146, 2021.

[10] A. Oymak and M. R. Tur, "A Short Review on the Optimization Methods Using for Distributed Generation Planning," International Journal of Smart Grid-ijSmartGrid, vol. 6, no. 3, pp. 54-64, 2022.

[11] R. Khezri, A. Mahmoudi, and M. H. Haque, "Optimal Capacity of Solar PV and Battery Storage for Australian Grid-Connected Households," EEE Transactions on Industry Applications, vol. 56, no. 5, pp. 5319-5329, 2020.

[12] J. Ma and X. Ma, "Distributed Control of Battery Energy Storage System in a Microgrid," in 2019 8th International Conference on Renewable Energy Research and Applications (ICRERA), IEEE, pp. 320-325, 2019.

[13] M. S. Islam, N. Mithulananthan, K. Bhumkittipich, and A. Sode-Yome, "EV Charging Station Design with PV and Energy Storage Using Energy Balance Analysis," in 2015 IEEE Innovative Smart Grid Technologies-Asia (ISGT ASIA), pp. 1-5, 2015.

[14] N. M. Kumar, J. Vishnupriyan, and P. Sundaramoorthi, "Techno-Economic Optimization and Real-Time Comparison of Sun Tracking Photovoltaic System for Rural Healthcare Building," Journal of Renewable Sustainable Energy, vol. 11, no. 1, p. 015301, 2019.

[15] Y. Wang, M. Kazemi, S. Nojavan, and K. Jermsittiparsert, "Robust Design of Off-Grid Solar-Powered Charging Station for Hydrogen and Electric Vehicles Via Robust Optimization Approach," International Journal of Hydrogen Energy, vol. 45, no. 38, pp. 18995-19006, 2020.

[16] H. Jin, S. H. Nengroo, S. Lee, and D. Har, "Power Management of Microgrid Integrated with Electric Vehicles in Residential Parking Station," in 10th International Conference on Renewable Energy Research and Application (ICRERA), IEEE, pp. 65-70, 2021.

[17] L. Grande, I. Yahyaoui, and S. Gómez, "Energetic, Economic and Environmental Viability of Off-Grid PV-BESS for Charging Electric Vehicles: Case Study of Spain," Sustainable cities and society, vol. 37, pp. 519-529, 2018.

[18] J. Ugirumurera and Z. J. Haas, "Optimal Capacity Sizing for Completely Green Charging Systems for Electric Vehicles," IEEE Transactions on Transportation Electrification, vol. 3, no. 3, pp. 565-577, 2017.

[19] O. Ekren, C. H. Canbaz, and Ç. B. Güvel, "Sizing of a Solar-wind Hybrid Electric Vehicle Charging Station by Using HOMER Software," Journal of Cleaner Production, vol. 279, p. 123615, 2021.

[20] H. Sánchez-Sáinz, C.-A. García-Vázquez, F. Llorens Iborra, and L. M. Fernández-Ramírez, "Methodology for the Optimal Design of A Hybrid Charging Station of Electric and Fuel Cell Vehicles Supplied by Renewable Energies and An Energy Storage System," Sustainability, vol. 11, no. 20, p. 5743, 2019.

[21] D. Sadeghi, A. Naghshbandy, and S. Bahramara, "Optimal Sizing of Hybrid Renewable Energy Systems in Presence of Electric Vehicles Using Multi-objective Particle Swarm Optimization," Energy, vol. 209, p. 118471, 2020.

[22] A. Al Wahedi and Y. Bicer, "Techno-economic Optimization of Novel Stand-alone Renewables-based Electric Vehicle Charging Stations in Qatar," Energy, vol. 243, p. 123008, 2022.

[23] A. Abdulla and B. Yusuf, "Development of an Off-Grid Electrical Vehicle Charging Station Hybridized with Renewables Including Battery Cooling System and Multiple Energy Storage Units," Energy Reports, vol. 6, pp. 2006-2021, 2020.

[24] U. Akram, M. Khalid, and S. Shafiq, "An Improved Optimal Sizing Methodology for Future Autonomous Residential Smart Power Systems," IEEE Access, vol. 6, pp. 5986-6000, 2018.

[25] M. Ban, D. Guo, J. Yu, and M. Shahidehpour, "Optimal Sizing of PV and Battery-Based Energy Storage in An Off-Grid Nanogrid Supplying Batteries to A Battery Swapping Station," Journal of Modern Power Systems and Clean Energy, vol. 7, no. 2, pp. 309-320, 2019.

[26] "Power Data Access Viewer NASA. Avaliable: https://power.larc.nasa.gov/data-access-viewer/."

[27] A. Z. Gabr, A. A. Helal, and N. H. Abbasy, "Economic Evaluation of Rooftop Grid-Connected Photovoltaic Systems for Residential Building in Egypt," International Transactions on Electrical Energy Systems, vol. 30, no. 6, p. e12379, 2020.

[28] A. A. Nafeh, "Optimal Economical Sizing of A PV-Wind Hybrid Energy System Using Genetic Algorithm," International Journal of Green Energy, vol. 8, no. 1, pp. 25-43, 2011.

[29] A. Hassan, Y. M. Al-Abdeli, M. Masek, and O. Bass, "Optimal Sizing and Energy Scheduling of Grid-Supplemented Solar PV Systems with Battery Storage: Sensitivity of Reliability and Financial Constraints," Energy, vol. 238, p. 121780, 2022.

[30] A. A. Nafeh, "Design and Economic Analysis of A Stand-Alone PV System to Electrify a Remote Area Household in Egypt," The open renewable energy journal, vol. 2, no. 1, 2009.

[31] M. M. Samy, M. I. Mosaad, M. F. El-Naggar, and S. Barakat, "Reliability Support of Undependable Grid Using Green Energy Systems: Economic Study," IEEE Access, vol. 9, pp. 14528-14539, 2020.

[32] S. B., M. Chandra, Q. Zian, E. Ramirez, and B. Pavol, "Techno-Economical Model Based Optimal Sizing of PV-Battery Systems for Microgrids," IEEE Transactions on Sustainable Energy, vol. 11, no. 3, pp. 1657-1668, 2019.

[33] A. Karmaker, M. Ahmed, M. Hossain, and M. Sikder, "Feasibility Assessment & Design of Hybrid Renewable Energy Based Electric Vehicle Charging Station in Bangladesh," Sustainable cities and society, vol. 39, pp. 189-202, 2018.

[34] A. A. Omran, F. H. Fahmy, A. A. Nafeh, and H. K. Yousef, "Sizing, Modeling and Control of Photovoltaic

Traffic Light System," IOSR J. Electr. Electron. Eng, vol. 11, no. 6, pp. 25-36, 2016.

[35] Q. Dai, J. Liu, and Q. Wei, "Optimal Photovoltaic/Battery Energy Storage/Electric Vehicle Charging Station Design Based on Multi-Agent Particle Swarm Optimization Algorithm," Sustainability, vol. 11, no. 7, p. 1973, 2019.

[36] T. M. E. Abou Saltouh, A. A. Nafeh, A. A. Abou El-Ela, F. H. Fahmy, and S. K. Nawar, "Control Strategy for Seamless Transition Between Grid-Connected and Islanding Modes in Microgrid-Based PV Inverters," Energy Systems, pp. 1-28, 2022.

[37] M. Azaroual, M. Ouassaid, and M. Maaroufi, "An Optimal Energy Management of Grid-Connected Residential Photovoltaic-Wind-Battery System Under Step-Rate and Time-Of-Use Tariffs," International Journal of Renewable Energy Research, vol. 10, no. 4, 2020.

[38] A. K. Karmaker, M. R. Ahmed, M. A. Hossain, and M. M. Sikder, "Feasibility Assessment & Design of Hybrid Renewable Energy Based Electric Vehicle Charging Station in Bangladesh," Sustainable cities and society, vol. 39, pp. 189-202, 2018.

[39] F. A. Hashim and A. G. Hussien, "Snake Optimizer: A Novel Meta-heuristic Optimization Algorithm," Knowledge-Based Systems, vol. 242, p. 108320, 2022.

[40] M. Tostado-Véliz, D. Icaza-Alvarez, and F. Jurado, "A Novel Methodology for Optimal Sizing Photovoltaic-Battery Systems in Smart Homes Considering Grid Outages and Demand Response," Renewable Energy, vol. 170, pp. 884-896, 2021.

[41] Egypt Interest Rate, . Available: https://tradingeconomics.com

[42] R. Ashique, Z. Salam, M. Aziz, and A. Bhatti, "Integrated Photovoltaic-Grid DC Fast Charging System for Electric Vehicle: A Review of The Architecture and Control," Renewable Sustainable Energy Reviews, vol. 69, pp. 1243-1257, 2017.